



PHASE 1 FINAL REPORT
 Contract #: N00014-94-C-0216
 Item #: 0001AC

ERBIUM DOPED SILICON LEDs USING IC COMPATIBLE PROCESSING

Accession For	
NTIS CRA&I	<input checked="" type="checkbox"/>
DTIC TAB	<input type="checkbox"/>
Unannounced	<input type="checkbox"/>
Justification	
By <i>per ltr</i>	
Distribution /	
Availability Codes	
Dist	Avail and/or Special
A-1	

Submitted To:
 Office of Naval Research
 Code 251B KIJ
 Ballston Tower One
 800 North Quincy Street
 Arlington, VA 22217-5660

DISTRIBUTION STATEMENT A
 Approved for public release
 Distribution Unlimited

Submitted By:
 Implant Sciences Corporation
 107 Audubon Road
 #5 Corporate Place
 Wakefield, MA 01880

19950926 001

DTIC QUALITY INSPECTED 1

Table of Contents

1.0	Introduction and Summary	4
2.0	Background Technology	6
3.0	Technical Results	8
3.1	Experimental	8
3.2	Sample Preparation for Annealing Studies	9
3.3	Annealing Conditions and Characterization	10
3.4	Device Fabrication	13
3.5	Device Evaluation	15
4.0	Suggestions for Continued Research	23

List of Tables

Table 1.	Er Anneal Study Test Matrix.
Table 2.	Process Flow Comparison: Lots 1 & 2.

List of Figures

- Figure 1. Implanted depth distribution as predicted by Profile Code™ for nominally 400 keV Er and O codopant at 2:1 atomic concentration ratio.
- Figure 2. Photoluminescence intensities of Er with various codopants at $T = 4.2$ K. A.) After 800 °C, 30 min. anneal, B.) After 900 °C, 30 min. anneal.
- Figure 3. SIMS profiles of Er/F sample as implanted and post anneal.
- Figure 4. Schematic cross section of a surface-emitting 400 keV Si:Er LED. The peak concentration of Er/O was $5 \times 10^{17} \text{ cm}^{-3} / 2 \times 10^{18} \text{ cm}^{-3}$ at a peak depth of 1500 Å. The n+ emitter was formed by arsenic implantation, and the back side p+ region was boron implanted.
- Figure 6. Schematic illustration of the PL/EL test apparatus.
- Figure 5. SEM image of a mesa-isolated surface-emitting 400 keV Si: Er LED.
- Figure 7. Typical I-V characteristics of a surface-emitting 400 keV Si: Er LED.
- Figure 8. Leakage current wafer mapping of a diode from Lot 1.
- Figure 9. Electroluminescence spectrum of a 400 keV Si: Er LED at 100K.
- Figure 10. Electroluminescence spectrum of a 400 keV Si: Er LED at room temperature.
- Figure 11. Er^{3+} electroluminescence intensity ($\lambda = 1.54 \mu\text{m}$) from both a 400 keV Si: Er LED and a 4.5 MeV Si: Er LED vs. drive current density at 100K.
- Figure 12. Er^{3+} electroluminescence intensity ($\lambda = 1.54 \mu\text{m}$) from both a 400 keV Si: Er LED and a 4.5 MeV Si: Er LED vs. drive current density at room temperature.
- Figure 13. Temperature dependence of Er^{3+} electroluminescence intensity ($\lambda = 1.54 \mu\text{m}$) from a 400 keV Si: Er LED.
- Figure 14. Shallow arsenic emitter depth dependence of Er^{3+} electroluminescence intensity ($\lambda = 1.54 \mu\text{m}$).

1.0 Introduction and Summary

This Final Report describes the technical approach and research effort during the Phase I STTR program. The purpose of the program is to demonstrate the capability of the IC compatible process technology of rare earth ion implantation for the integration of photonic interconnection with silicon based electronics. The objective of the Phase I research was to fabricate a simple light emitting device using low energy ($< 1\text{MeV}$) rare earth ion implantation. Room temperature emission at the characteristic wave length of $1.54\text{ }\mu\text{m}$ was observed at room temperature. Additionally, many of the performance characteristics of the IC compatible 400 keV Er implanted LED's exceed those fabricated using more difficult and costly MeV implantation¹. Results from LED's fabricated using 400 keV implants during this program as compared to 4.5 MeV implants performed in earlier work clearly illustrate the following;

- 7.4 times increase in internal quantum efficiency.
- I_{sat} achieved at lower drive current densities.
- 3.6 times increase in external quantum efficiency.

Erbium luminescence in silicon is directly related to the annealing cycle as shown by earlier work performed at MIT with high energy implantation ($\sim 4.5\text{MeV}$). Additionally, species such as N, F, C and O have produced more intense emission when co-implanted with erbium. Accordingly, the first step of this effort was to determine optimal annealing conditions for the more shallow low energy implants co-doped with various other elements. Over 200 wafer implant steps were performed during the phase I effort as part of a test matrix examining; Er implant energy (range), co-dopant species, co-dopant dose ([Er/co-dopant]), anneal temperature, and anneal time. After determining optimal implant and anneal conditions the first set of device wafers was begun. Initially, the objective was to stimulate emission using photoluminescence then electroluminescence at cryogenic temperatures. As a result of the encouraging data collected from the first device lot a second lot was begun in an attempt to stimulate both modes of emission at higher temperatures and, with hope, room temperature.

The desire to use silicon for optoelectronic devices is fueled by its low cost and high integration capability. This provides the potential to increase the speed of data transfer and reduces the need of metallic interconnects. One of the crucial components for photonics applications is a silicon lightsource that can be driven by standard MOSFET's. The first Si LEDs operating at room temperature have been demonstrated by using the luminescence of erbium, implanted in silicon. The erbium implants were performed at an energy of about 5 MeV with an implanter that is not commonly used in silicon processing lines. Standard implanters can provide a maximum acceleration energy of nominally 400 keV for doubly charged erbium. Consequently the erbium dose for these implants with identical peak concentration is about 20 times smaller, and therefore is expected to decrease the luminescence intensity by the same factor. The challenge in this project was to overcome this disadvantage and demonstrate room temperature performance using shallow 400 keV erbium implants.

Several steps were necessary to achieve this goal: (1) define the processing window for the annealing steps from scratch since a shallow implant favors out-diffusion of the co-implanted light elements; (2) the temperature dependence of several erbium-ligand systems had to be studied to optimize the luminescence intensity at room temperature; (3) the shallow erbium implant with an implantation depth of 1500Å requires an unusually shallow junction to avoid overlap with the erbium implant.

Fluorine, carbon, oxygen, and nitrogen were chosen as erbium ligands since they were already known to enhance the Er luminescence. In addition to these elements, selenium and chlorine were used as co-dopants to study if elements with low diffusivity are advantageous for shallow implants. The samples were annealed at 800°C and 900°C for 30 min. The greatest luminescence intensity at LHe temperature was observed for oxygen co-implanted samples. Measurements at that temperature reveal implantation related damage not removed by the annealing step. The spectral features for most samples were identical. Measurements on deep Er implants showed that different co-implants have characteristic spectral features which were missing for the shallow implants. SIMS profiles revealed that the co-implanted elements except O, Cl and Se were out-diffused during the annealing process. To compensate for out-diffusion, a triple implant at three different energies for the co-implanted elements was used to completely saturate the Er peak in co-dopant instead of simply making the peaks coincident. Consequently due to the higher dose, more erbium-ligand complexes are expected to form and prevent complete out-diffusion.

The second thorough study focused on the temperature dependence of the erbium luminescence intensity. The erbium luminescence decreases with increasing temperature. This decay depends strongly on the annealing conditions, the residual implantation damage and the co-implanted element. It was observed that oxygen co-implants at a peak concentration of $2 \times 10^{18} \text{cm}^{-3}$, annealed at 800°C show the highest PL intensity from LHe to room temperature. Furthermore the decay for a Se co-implant, annealed at 900°C is smaller than for any other co-implant and the PL intensity at room temperature is comparable with the highest intensity measured.

Based on our observations, an Er/O implant was chosen for the first generation of LEDs. A standard 25 keV arsenic implant and subsequent rapid thermal anneal (RTA) to form a shallow n+/p junction was used. As expected the junction depth proved to be a critical factor in the LED performance. Spreading resistance measurements placed the junction in the erbium region although the results of SUPREM 3 simulations placed the junction at a shallower depth. By using different annealing times the junction depth was varied. It was determined that the electroluminescence intensity increases with decreasing junction depth. We believe that because of the overlap of arsenic and erbium, the LED emission intensity is small and not measurable at room temperature.

For the second generation LEDs, an arsenic implant at 10 keV was chosen to decrease the junction depth even further, and the total thermal budget was reduced by reducing the annealing steps. These LEDs produced room temperature Er luminescence despite the fact that the diode leakage current was more than 5 orders of magnitude higher than for comparable deep implanted Er LEDs. The external quantum efficiency improved by a factor of 3.5 compared with previous deep implanted LEDs. The high leakage current shows that the processing is still far from optimized and there is a need to develop the ability to make a good shallow junction contact for this process.

The fabrication of room temperature LEDs based on the Si-Er system using the IC compatible process of ion implantation was successfully accomplished. Although several conditions are not yet optimized, the quantum efficiency of these LEDs already supersedes the quantum efficiency of LEDs made by deep Er implants. The key findings for shallow implants are that out-diffusion plays a major role and, therefore, lower process temperatures are necessary. Preliminary results for triply charged Er, implanted at 600 keV, show some improvement ($\sim 20\%$ more light output) over the 400 keV implants. 600 keV Er implants allow deeper p-n junctions. The p-n junction depth is a major concern for the performance of the LEDs. A third generation LED is currently being processed with a phosphorus doped polysilicon as top n+ emitter instead of As implant to achieve an even shallower n+/p junction. Improvement of the emission intensity is anticipated from the optimization of the junction. Additional improvement is expected by performing multiple energy Er implants to increase the volume of active Er color centers.

In summary, room temperature electroluminescence from shallow erbium implants was successfully achieved. The resulting devices exhibited superior internal and external quantum efficiencies and saturation currents were achieved at lower drive current densities. There is much room for improvement that should push this technology to maturity and make it applicable for use in VLSI technology.

2.0 Background Technology

Each succeeding integrated circuit technology follows distinct trends which stress interconnect performance. Currently, electronic interconnection using aluminum lines is pervasive. The trade-off is chip area and power consumption for speed. For example, a recently announced microprocessor chip supports a 200 MHz clock speed with a 2 cm^2 area dissipating 30 W. Approximately 3.5 nanofarads of capacitance (15% of the chip area) and 6.5 W of power are required to drive only the on-chip clock signal distribution. Other applications include; on-chip data transfer, direct chip to chip interconnection, driving a fiber optic cable and multiplexing directly without the use of a discrete III-V device.

As chips are getting larger, interconnects are getting smaller and more closely spaced. The current densities carried by aluminum lines have increased to values where reliability constraints, such as electromigration and stress migration, determine design as opposed to electrical performance. Word size has increased, requiring that more and more inputs and outputs be driven in parallel. These trends are pushing electrical interconnects to physical limits. Integrated microphotonic clock distribution and data I/O offer a solution to the interconnection bottleneck by providing high bandwidth links which can have submicron widths and spacings with negligible crosstalk, and which are free of resistance, capacitance and reliability limitations.

The alternative materials systems to address the interconnection bottleneck are as follows; 1) Aluminum interconnects are limited primarily by reliability issues: electromigration and stress voiding, particularly at high power with fine lines. 2) Copper interconnects have low resistance and unknown reliability. Processing (dry etching) needs development. All electronic interconnection is ultimately limited by cross talk. 3) Hybrid photonic interconnection based on III-V semiconductors is a discrete technology. Alignment and testing costs are prohibitive for high levels of integration (although an off-chip laser source for clock distribution with integrated SiO₂ waveguides and Si pin detectors is a contender). Heteroepitaxy (GaAs on Si) is not yet compatible with the defect requirements for high levels of integration. 4) Porous (quantum) silicon is not compatible with planarity requirements for integration.

The most appropriate solution is to employ erbium-doped silicon light emitters, silicon based waveguides, and silicon based detectors to provide an IC compatible process technology. This allows the possibility of integrated switching, modulation, coupling, and micromachined external waveguide connection to be addressed. The Er:Si electroluminescent devices emit at $\lambda = 1.54 \mu\text{m}$. This wavelength is compatible with telecommunication standards and, since $h\nu < E_g$, the photons do not affect standard silicon electronics (eg. empty a DRAM cell). Er:Si does not contaminate high purity gate oxidation furnaces and is thus compatible with clean room processing. The bandwidth of the Er:Si photon is $\sim 10^{15}$ Hz, and it does not introduce propagation delay as resistance and capacitance of metal lines do. The silicon optical circuit has no known reliability limitations. Si, SiO₂ and SiGe provide all the materials needs for photon generation, confinement and detection. New capabilities introduced by silicon microphotonics include: i) parallel architectures with multiplexing, reduced clock speeds and concurrent operations, ii) immunity from electromagnetic interference, shorts and ground loops, and ignition of combustibles, and iii) package integration.

The use of erbium in silicon as a light emitter was first demonstrated by Ennen et al². These early experiments showed the potential of this defect system as a building block of silicon optoelectronics. In spite of this potential, systematic studies on erbium in silicon were started about 15 years after its discovery. It was found that ligands play a key role in the optical activation of erbium in silicon. While erbium in floatzone silicon (with an oxygen and carbon background contamination of $< 10^{16} \text{ cm}^{-3}$) is not optically active, co-doping with oxygen, carbon, nitrogen or fluorine enhance the luminescence significantly. This enhancement is due to the

formation of erbium-ligand complexes. The erbium solubility in silicon is very low ($\sim 10^{16} \text{ cm}^{-3}$ at 1300°C) so that nonequilibrium techniques had to be employed in order to introduce high amounts of erbium into the substrate. The technique that produced the most promising results is ion implantation. Special high energy implanters were used to implant erbium at 5.25 MeV with the peak concentration at $1.8 \mu\text{m}$ depth. The introduced lattice damage had to be removed by annealing at temperatures around 900°C . Experiments showed that it is very important to understand the erbium-ligand formation and dissociation in order to find optimum annealing conditions. These conditions depend mainly on the ligands and the implantation depth. For deep implants the optimum luminescence yield for an oxygen co-implant was obtained with a 900°C , 30 min anneal.

The room temperature performance of Si:Er LEDs was demonstrated using high MeV deep erbium implants. The 4.5MeV Si:Er LEDs were fabricated in a class 10 clean room at MIT using standard VLSI compatible technique. The LED structure is essentially a mesa-isolated, oxide-passivated p/n junction. The p/n junction is close to the implanted Er region and minority carriers are injected into the Er region in forward bias to excite Er and emit light.

3.0 Technical Results

3.1 Experimental

All Er implants were performed at Implant Sciences Corporation (ISC) on a heavily modified Lintott 200keV implanter using a modified chlorination ion source design³. Over 100 Er wafer-implant steps were performed during the phase I effort. Er implants were performed at nominally 200, 400 and 600 keV. Co-dopant implants were performed on an Eaton 3206 production implanter. Depth distributions were modeled using Profile CodeTM. Co-dopant energies were selected to place the peak coincident with the Er peak. As implants to form very shallow junctions were also performed on the Eaton 3206 with an additional high voltage power supply connected in reverse polarity to the post-acceleration column. Over 100 co-dopant and shallow junction wafer-implant steps were performed during the phase I effort. Implant Sciences maintains class 100 clean rooms in its semiconductor implant area.

400 keV Si:Er LEDs were fabricated in Microsystems Technologies Laboratories (MTL) at MIT. The facility is a class 10 clean room running a $1.5 \mu\text{m}$ CMOS baseline process on 4" silicon wafers. The main fabrication tools used includes: RCA clean station, rapid thermal anneal station, thermal anneal tube, low temperature oxide deposition (LPCVD) tube, metal sinter tube, photolithography equipment, plasma etching equipment, metal sputtering deposition equipment, wet acid station, and ion implanter.

Photoluminescence (PL) experiments were conducted by using an Ar ion laser for excitation. Electroluminescence (EL) measurements were performed by applying a forward bias to the diode with a pulse generator. The emitter radiation was dispersed using a 0.75m Spex monochromator and detected by a liquid nitrogen cooled Northcoast Ge detector. Low temperature and temperature dependence measurement were performed by mounting the LED in an Oxford helium cryosystem (CF204).

3.2 Sample Preparation for Annealing Studies

Earlier work concerning rare earth doping of ZnS and ZnSe for electroluminescent display purposes led to an initial design of a Freeman type ion source which produced relatively abundant rare earth ion beams, including double and triple charge states. The source was optimized for erbium generation. It was eventually discovered that more than adequate beam current could be generated to perform the low dose implants, but cleanliness of the spectra was in question. Steel heat shields and the gas feed line contributed unwanted contaminant peaks to the spectra. Fe-54 in particular, lay directly under the Er^{+++} peak. Most ion sources use stainless steel tubing for introducing the feed gas into the hot arc chamber and occasionally for heat shields. Since the host material of Si, unlike ZnS or ZnSe, is sensitive to poisoning, any Fe containing components in the hot region near the arc chamber had to be eliminated. Additionally the arc chamber itself and its surrounding ceramic thermal blanket was redesigned to provide better insulation. Finally, the crucible was modified to provide for more efficient chlorination of the Er charge and better transfer of the vaporized chloride into the arc chamber.

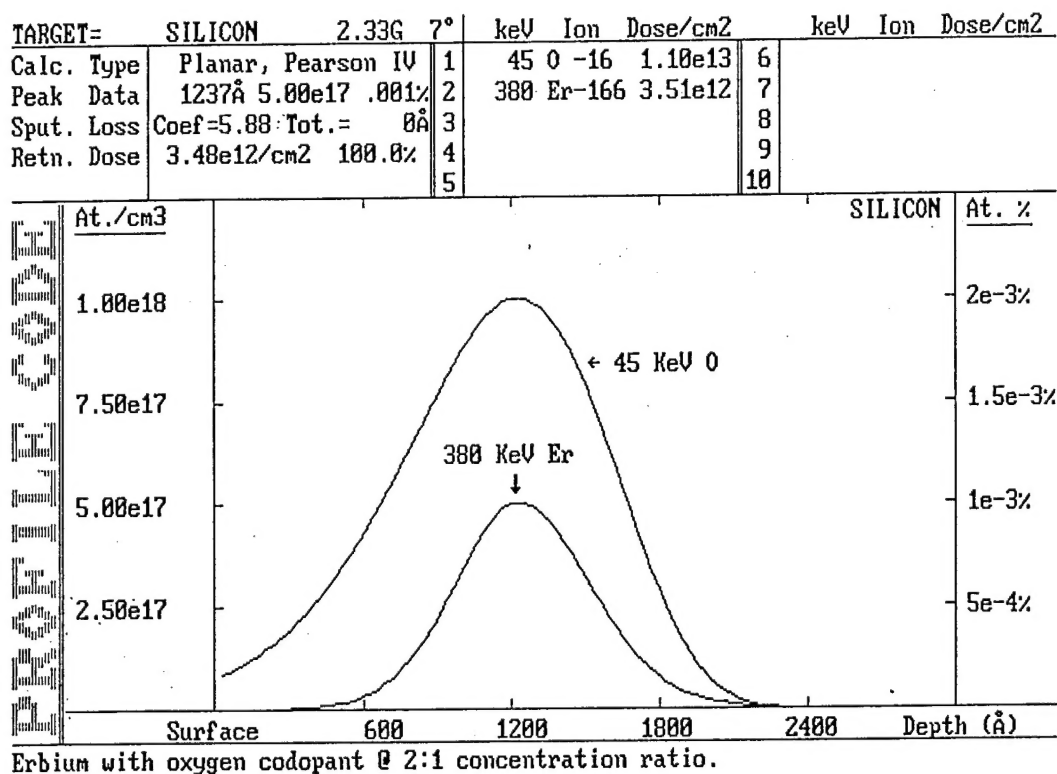
In order for the co-dopant to have an effect on Er emission it must occupy the same volume as the Er. Dose and energy parameters were determined with the use of Profile CodeTM to produce coincident peaks. Profile CodeTM is a commercial software package which uses a semi-empirical calculation to model implant depth distributions⁴. The Er dose was determined to yield a peak atomic concentration of $5 \times 10^{17} \text{cm}^{-3}$ at 200, 400 and 600 keV. The energy of the co-dopant species was chosen so that the peaks coincide. Co-dopant dose was modeled so that its atomic concentrations was either 2X or 4X that of Er. Fluorine, chlorine, oxygen, selenium, nitrogen, and carbon were implanted as co-dopants to provide a ligand field to enhance emission to atomic concentrations of 1.0 and $2.0 \times 10^{18} / \text{cm}^3$. An example output of a final depth distribution as modeled for nominally 400 keV Er co-doped with oxygen is given in Fig. 1.

An extensive sample matrix was studied. The matrix consisted of the following; 3 Er implant energies, 6 co-dopant species, 2 co-dopant atomic concentration ratios to Er, 3 anneal temperatures and 3 anneal durations. 324 samples were examined for PL and EL output at various temperatures. Additionally, about 30 samples were tested to determine the effect of rapid thermal annealing (RTA). Table One contains all of the implant combinations of Er and co-dopants and their implant parameters. The substrates were 4" $p < 100 >$ Czochralski grown (CZ) wafers. All implants were performed at 7° incidence, and no beam current limitations were required due to the relatively low doses involved.

3.3 Annealing Conditions and Characterization

Previously, no annealing experiments for low keV erbium implants were reported. Therefore it was necessary to find the optimum annealing window for maximum luminescence output. Because of the shallow implantation it was expected that the co-dopants would out-diffuse at a much higher rate than for deep implants. We constructed a matrix to study the PL intensity for several co-implants at different annealing temperatures. The results were used to define the processing conditions and most effective co-implants for the LEDs.

Fig. 2a and b show the PL intensities at LHe temperature of Er after co-implantation of different elements at two anneal temperatures. These elements were chosen because previous studies show enhancement of the Er luminescence due to the incorporation of these elements. Oxygen, fluorine, carbon and nitrogen enhance the Er luminescence significantly by forming Er-ligand complexes. Cl and Se are heavier than the previous elements and have a slow diffusion rate in silicon. The diffusion rate determines the loss due to out-diffusion at the



Erbium with oxygen codopant @ 2:1 concentration ratio.

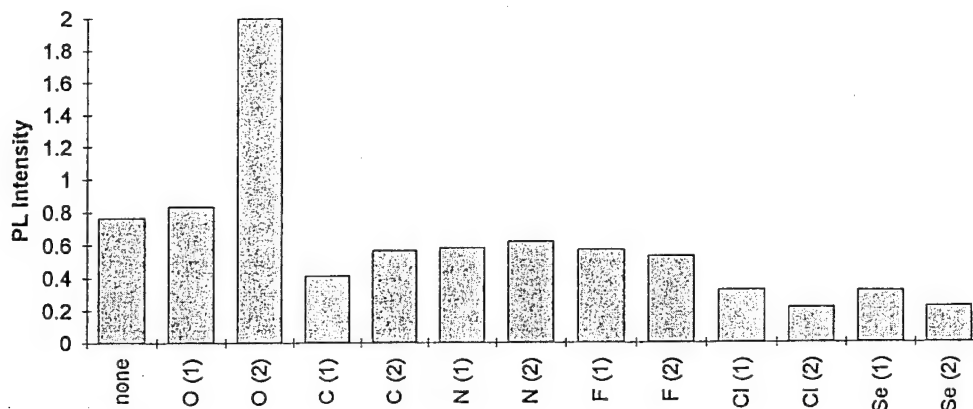
Figure 1. Implanted depth distribution as predicted by Profile Code™ for nominally 400 keV Er and O codopant at 2:1 atomic concentration ratio.

Table One

Erbium Anneal Study Test Matrix

Boat #, Lot ID	Wafer		Erbium		Co-Dopant				Conc. Ratio [Er/C/D.]
	Pos.	ID #	Energy (keV)	Dose ($\times 10^{12}/\text{cm}^2$)	Species	Energy (keV)	Dose ($\times 10^{13}/\text{cm}^2$)	Conc. ($\times 10^{19}/\text{cm}^3$)	
Boat #1, 2KLQA	1	AY D4	200 keV	2.20 $\times 10^{12}/\text{cm}^2$	F-19	34keV	0.70 $\times 10^{13}/\text{cm}^2$	1.0 $\times 10^{19}/\text{cm}^3$	1:2
	2	B5 B5	200	2.20	F-19	34	1.40	2.0	1:4
	3	B1 F6	200	2.20	N-14	28	0.70	1.0	1:2
	4	B2 C7	200	2.20	N-14	28	1.40	2.0	1:4
	5	AS E6	200	2.20	Cl-35	66	0.62	1.0	1:2
	6	AP G0	200	2.20	Cl-35	66	1.20	2.0	1:4
	7	AL C6	200	2.20	O-16	27	0.80	1.0	1:2
	8	AN E3	200	2.20	O-16	27	1.60	2.0	1:4
	9	CZ F0	200	2.20	Se-80	115	0.61	1.0	1:2
	10	CV B6	200	2.20	Se-80	115	1.22	2.0	1:4
	11	CT A1	200	2.20	C-12	24	0.74	1.0	1:2
	12	CS D0	200	2.20	C-12	24	1.48	2.0	1:4
	13	D1 E0	200	2.20	CONTROL	-----	-----	-----	----
	14	BS D7	600 keV	4.83 $\times 10^{12}/\text{cm}^2$	CONTROL	-----	-----	-----	----
	15	CJ G6	600	4.83	F-19	81	1.22 $\times 10^{13}/\text{cm}^2$	1.0 $\times 10^{19}/\text{cm}^3$	1:2
	16	CI C2	600	4.83	F-19	81	2.44	2.0	1:4
	17	CG A5	600	4.83	N-14	70	1.20	1.0	1:2
	18	CH F1	600	4.83	N-14	70	2.40	2.0	1:4
	19	CP E2	600	4.83	Cl-35	159	1.40	1.0	1:2
	20	CK D7	600	4.83	Cl-35	159	2.80	2.0	1:4
	21	CQ B3	600	4.83	O-16	66	1.30	1.0	1:2
	22	F9 B3	600	4.83	O-16	66	2.60	2.0	1:4
	23	HM B1	600	4.83	Se-80	285	1.20	1.0	1:2
	24	C9 E0	600	4.83	Se-80	285	2.40	2.0	1:4
	25	D7 B4	600	4.83	C-12	53	1.25	1.0	1:2
Boat #2, 2KLQA	14	EX B5	600	4.83	C-12	53	2.50	2.0	1:4
	1	CC F2	400 keV	3.51 $\times 10^{12}/\text{cm}^2$	F-19	57	.975 $\times 10^{13}/\text{cm}^2$	1.0 $\times 10^{19}/\text{cm}^3$	1:2
	2	DX C4	400	3.51	F-19	57	1.95	2.0	1:4
	3	G0 EZ	400	3.51	N-14	47	0.95	1.0	1:2
	4	AB C0	400	3.51	N-14	47	1.99	2.0	1:4
	5	EF B6	400	3.51	Cl-35	112	0.92	1.0	1:2
	6	EZ AZ	400	3.51	Cl-35	112	1.84	2.0	1:4
	7	B2 F7	400	3.51	O-16	45	1.10	1.0	1:2
	8	GJ D2	400	3.51	O-16	45	2.20	2.0	1:4
	9	FF A7	400	3.51	Se-80	200	0.96	1.0	1:2
	10	F2 G6	400	3.51	Se-80	200	1.92	2.0	1:4
	11	EZ D2	400	3.51	C-12	40	1.01	1.0	1:2
	12	EM D6	400	3.51	C-12	40	2.02	2.0	1:4
	13	D6 B3	400	3.51	CONTROL	-----	-----	-----	----

A.)



B.)

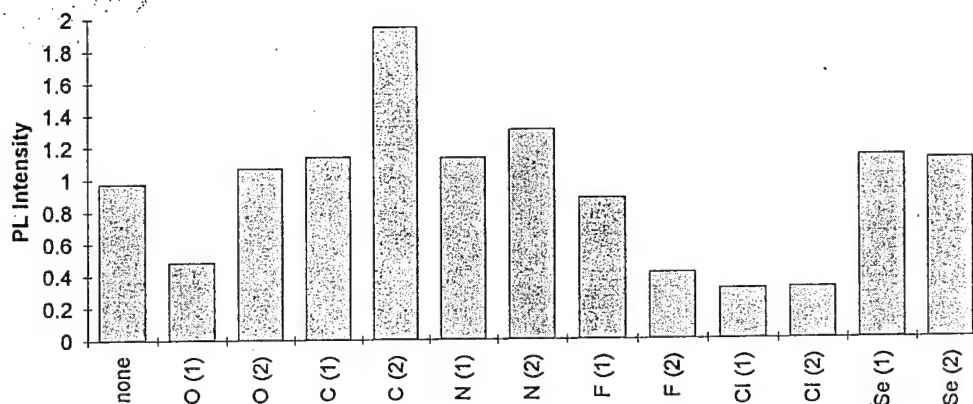


Figure 2. Photoluminescence intensities of Er with various codopants at $T = 4.2$ K. A.) After 800 °C, 30 min. anneal, B.) After 900 °C, 30 min. anneal.

surface. All samples were annealed at 800, 900 and 1000°C in a hot wall furnace in an Ar atmosphere. We conducted additional experiments using rapid thermal anneal (RTA). We found that RTA is not useful because the luminescence intensity for identical anneals varies by more than 20%. This variation is unacceptable for Si batch processing.

The anneals at 800°C for 30 min. show a maximum PL intensity for the O co-implanted sample (Fig. 2a), while the other co-implants show no improvement over Cz material without co-implant. SIMS measurement on an Er/F co-implanted and 800°C annealed sample revealed the out-diffusion of F due to the surface proximity. Fig. 3 shows the SIMS profiles of the sample as implanted and after the annealing step. The profiles show that fluorine is nearly completely out-diffused. The amount of F after annealing is therefore too small to enhance the Er luminescence. The PL intensity for a 900°C anneal is generally higher compared to the 800°C anneal (Fig. 2b). We attribute this increase to the improved lattice quality due to the higher annealing temperature. The highest luminescence intensity for the 900°C anneals was achieved by a C co-implant with a peak atomic concentration of $2 \times 10^{18} \text{ cm}^{-3}$.

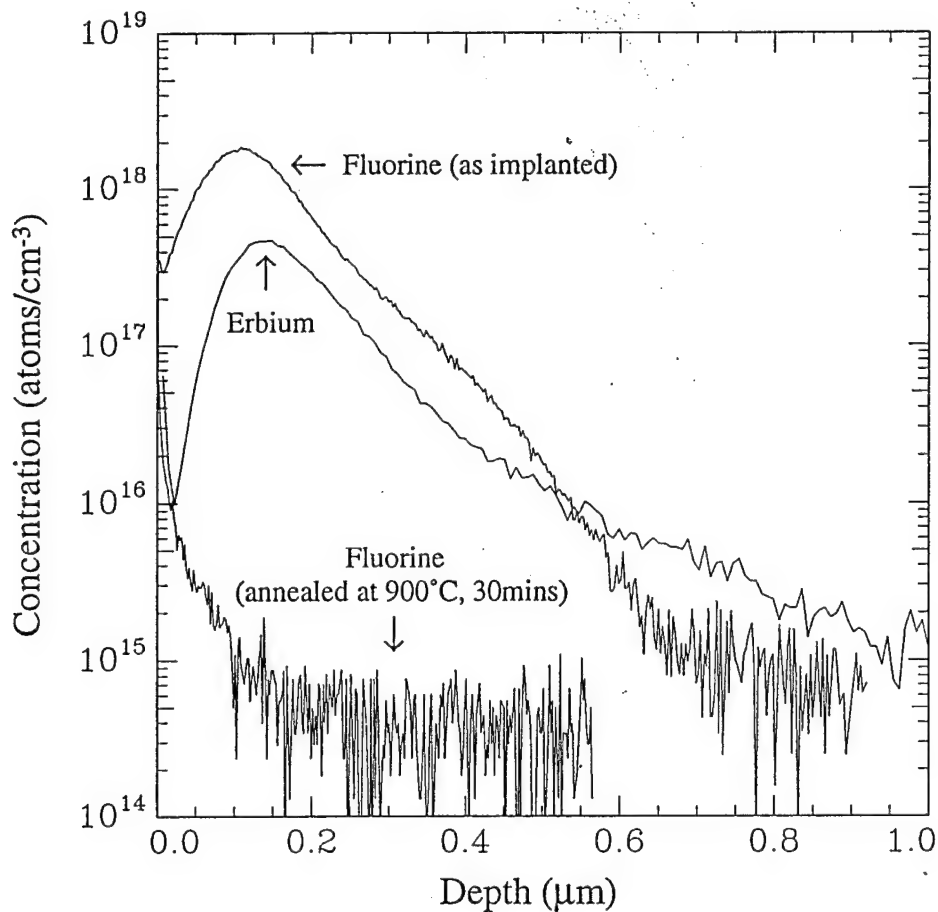


Figure 3. SIMS profiles of Er/F sample as implanted and post anneal.

3.4 Device Fabrication

Two lots of 400 keV Si:Er LEDs were designed and processed. Based on the test results of the first lot, the design of the second lot was improved and achieved room temperature operation of 400 keV Si:Er LEDs was achieved.

In lot 1, the substrate wafers were boron-doped p-type (100) oriented silicon CZ wafers (0.5 - 2 ohm·cm). Arsenic was implanted at an energy of 25 keV and a dose of $2 \times 10^{15} \text{ cm}^{-2}$ to form a n+/p junction. The backsides of the wafers were boron implanted to achieve good ohmic contacts. A rapid thermal annealing in nitrogen ambient (900 to 1100°C and 10s to 30s) was used to remove implantation damage and to activate the As dopant. Erbium was then implanted at an energy of nominally 400 keV with a peak atomic concentration of $5 \times 10^{17} \text{ cm}^{-3}$. An oxygen co-implant with a peak concentration of $2 \times 10^{18} \text{ cm}^{-3}$ was designed to spatially overlap the erbium implant. A heat treatment of 800°C for 30 min in N_2 was carried out to remove implantation damage and to optically activate erbium. Silicon mesas were defined by the first mask set and formed by plasma etching to provide electrical isolation among diodes. The surface was passivated by a low temperature oxide deposition at about 450°C. Contact openings were

defined by the second mask set and Al/Si was sputter deposited. A final photolithography step was followed by an Al/Si dry etch to define the LED metal contact pattern. A 400°C sinter in N₂/H₂ ambient annealed Al/Si contacts and completed the fabrication. A typical device cross section is shown in Fig. 4. Fig. 5 shows the SEM image of a surface emitting LED.

Er/O peak depth was at 1500Å from the surface as measured by SIMS. In the first lot, the projected arsenic depth was at 1000Å, but spreading resistance profiling measurement showed the existence of a junction at about 1500Å. We believe that most of the erbium implanted region was covered by a high concentration of $1 \times 10^{20} \text{ cm}^{-3}$ arsenic. The high As concentration dramatically decreases the minority carrier lifetime and therefore reduces the excitation efficiency for erbium. This leads to low electroluminescence intensity from the first lot. The quantitative EL intensity comparison will be shown in the next section.

Based on the first lot, a much shallower junction was needed to achieve high electroluminescence intensity. In the second lot, the same substrate wafers were used. Silicon mesas were formed first. Arsenic junction regions were defined by an extra photolithography step and the resist served as implant mask for both Er/O and As implants. Er and O were implanted at peak concentrations of $5 \times 10^{17} \text{ cm}^{-3}$ and $2 \times 10^{18} \text{ cm}^{-3}$ respectively and at a peak depth of 1500Å. A lower implant energy of 10 keV and a dose of $1 \times 10^{15} \text{ cm}^{-2}$ was used for the As junction. A heat treatment of 800°C/30min/N₂ was followed to activate both the arsenic electrical activity and the optical activity of erbium. The silicon surface was then passivated

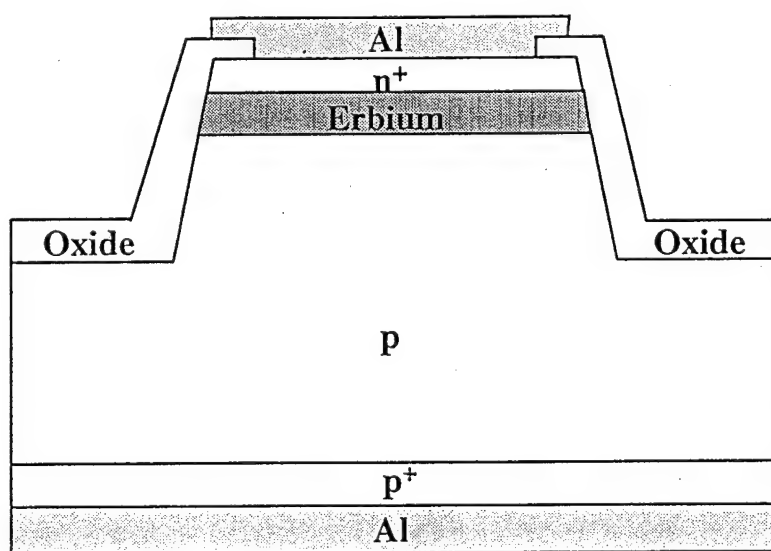


Figure 4. Schematic cross section of a surface-emitting 400 keV Si:Er LED. The peak concentration of Er/O was $5 \times 10^{17} \text{ cm}^{-3}$ / $2 \times 10^{18} \text{ cm}^{-3}$ at a peak depth of 1500 Å. The n+ emitter was formed by arsenic implantation, and the back side p+ region was boron implanted.

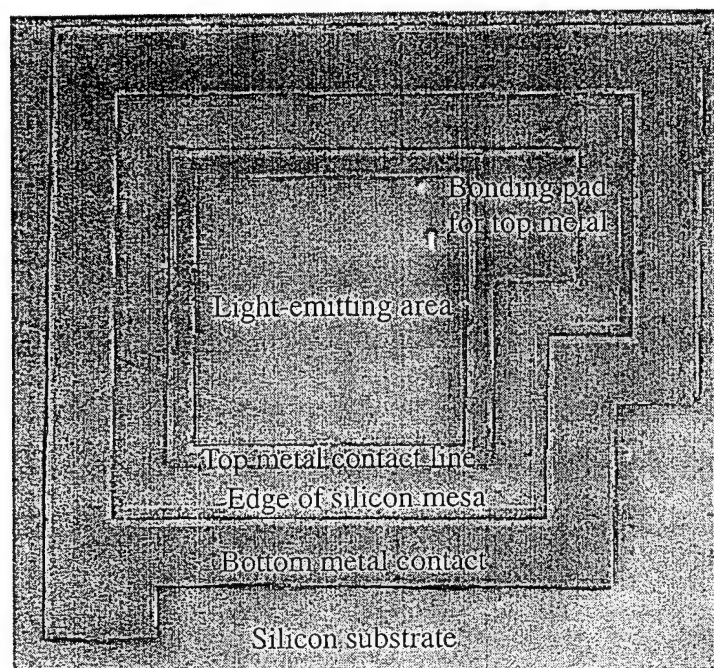


Figure 5. SEM image of a mesa-isolated surface emitting 400 keV Si:Er LED.

with low temperature oxide deposition. Since the simulated junction depth was only about 500\AA , Ti/Al/Si instead of Al/Si was deposited. The Ti layer, sandwiched between the Al/Si metal layer and the underlying contact open, is expected to alleviate shallow junction spiking problems. A step by step process flow comparison between two lots are shown in Table 2.

3.5 Device Evaluation

The experimental setup for emission measurement is shown in Fig. 6. Both photoluminescence (PL) and electroluminescence (EL) can be stimulated and measured at various temperatures. The two different excitation paths are shown. For photoluminescence experiments an Ar laser was used as excitation. Electroluminescence measurements were performed by applying a forward bias to an LED with a pulse generator. For low temperature and temperature dependant measurements the samples were mounted in an Oxford cryosystem (CF204). The temperature was varied between 4.2 K and 300 K (room temperature). The emission was dispersed using a 0.75 m SPEX monochromator and detected by a high sensitivity liquid nitrogen cooled Ge detector. The data were collected through a log-in amplifier onto a computer.

Table Two

Process Flow Comparison: Lots 1 & 2

Lot #1	Lot #2
As ⁺ Implant $2 \times 10^{15} \text{ cm}^{-2}$ @ 25 keV	Mesa Patteren
RTA (900 - 1100°C, 10-30 _s , N ₂)	Dry Etch
Er ⁺⁺ implant: $5 \times 10^{17} \text{ cm}^{-3}$, 400 keV	Implant pattern for As, Er, O
O ⁺ implant: $2 \times 10^{18} \text{ cm}^{-3}$, 45 keV	Er ⁺⁺ implant: $5 \times 10^{17} \text{ cm}^{-3}$, 400 keV
Anneal: 800°C, 30 min, N ₂	O ⁺ implant: $2 \times 10^{18} \text{ cm}^{-3}$, 45 keV
Mesa Pattern	As ⁺ implant: $1 \times 10^{15} \text{ cm}^{-2}$, 10 keV
Dry Etch	Anneal: 800°C, 30 min, N ₂
LTO Deposition	LTO Deposition
Contact Cut	Contact Cut
Al/Si Deposition	Al/Si Deposition
Al/Si Patteren and Etch	Al/Si Patteren and Etch
Sinter	Sinter

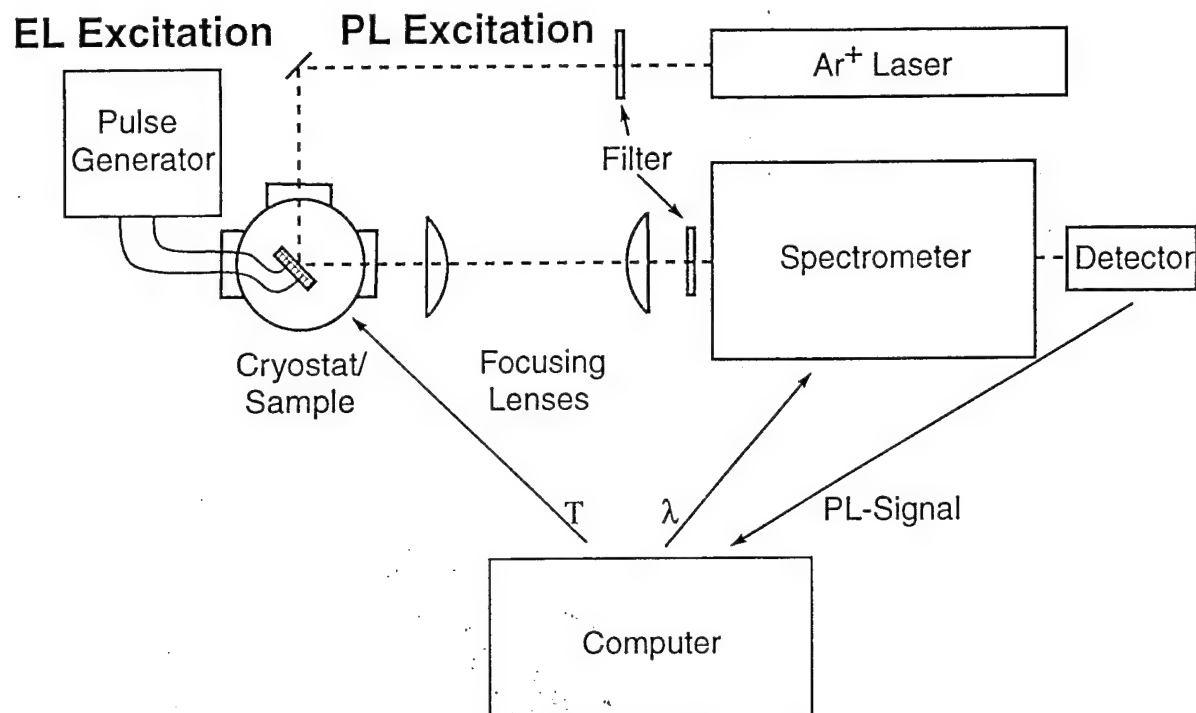
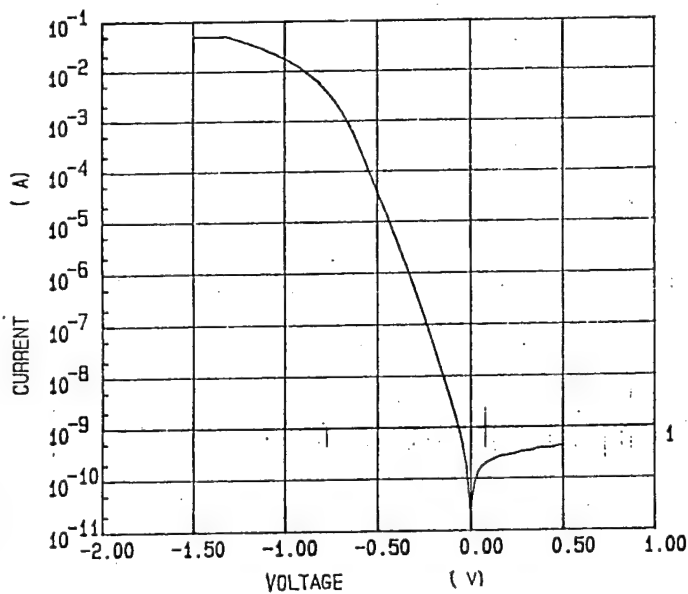


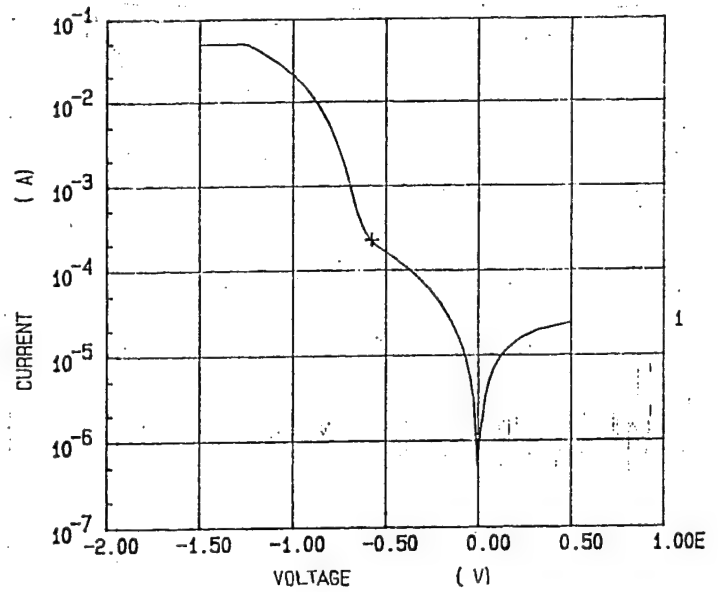
Figure 6. Schematic illustration of the PL/EL test apparatus.

Typical I-V characteristics of diodes from two lots are shown in Fig. 7. An ideality factor of 1.6 and 2.0 were observed in lot 1 and lot 2, respectively. Average leakage current densities were 1.3×10^{-6} A/cm² and 8.9×10^{-2} A/cm² for lot 1 and lot 2 at 5 V reverse bias. Diodes of the 2nd lot show more non-ideality behavior than diodes of the 1st lot. The higher leakage current in the 2nd lot may indicate junction spiking. More research is needed to improve the junction design and the shallow junction metal contacts. The leakage current wafer mapping from lot 1 is shown in Fig. 8. The variation of leakage current across the wafer is within normal distribution. The leakage current can be decreased by dry oxidation before the erbium implantation instead of low temperature oxide deposition to better passivate the silicon surface.

Fig. 9 and Fig. 10 show typical EL spectra for the shallow implanted LEDs from a surface-emitting Si:Er LED, observed at both 100 K and room temperature. A sharp linewidth ($\sim 150\text{\AA}$) at $\lambda = 1.54 \mu\text{m}$ is observed at room temperature. There are no obvious characteristic dislocation related D lines as observed in MeV Si:Er LEDs. This is due to the fact that 400 keV implantation introduces much less damage than 4.5 MeV implantation. The EL intensity



I-V of Lot 1 Diode



I-V of Lot 2 Diode

Figure 7. Typical I-V characteristics of a surface-emitting 400 keV Si: Er LED.

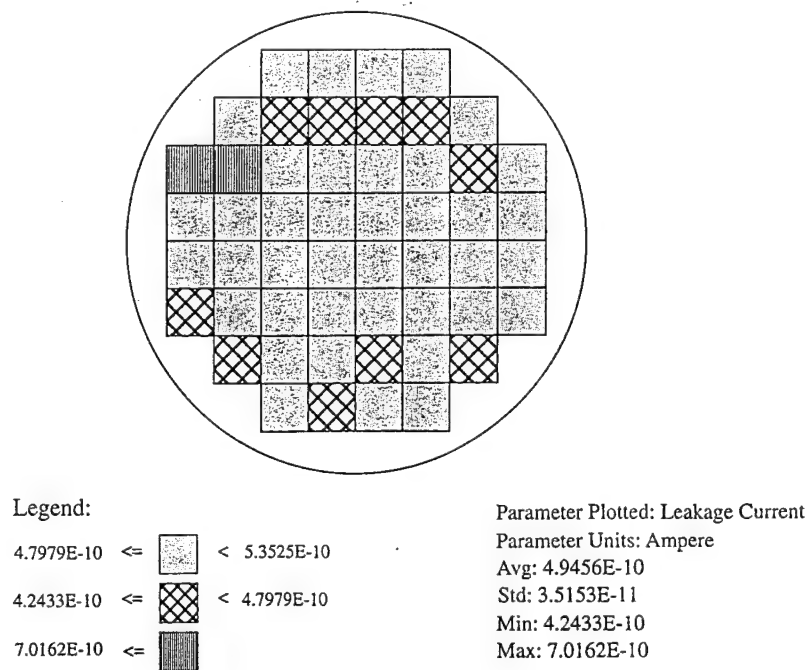


Figure 8. Leakage current wafer mapping of a diode from Lot 1.

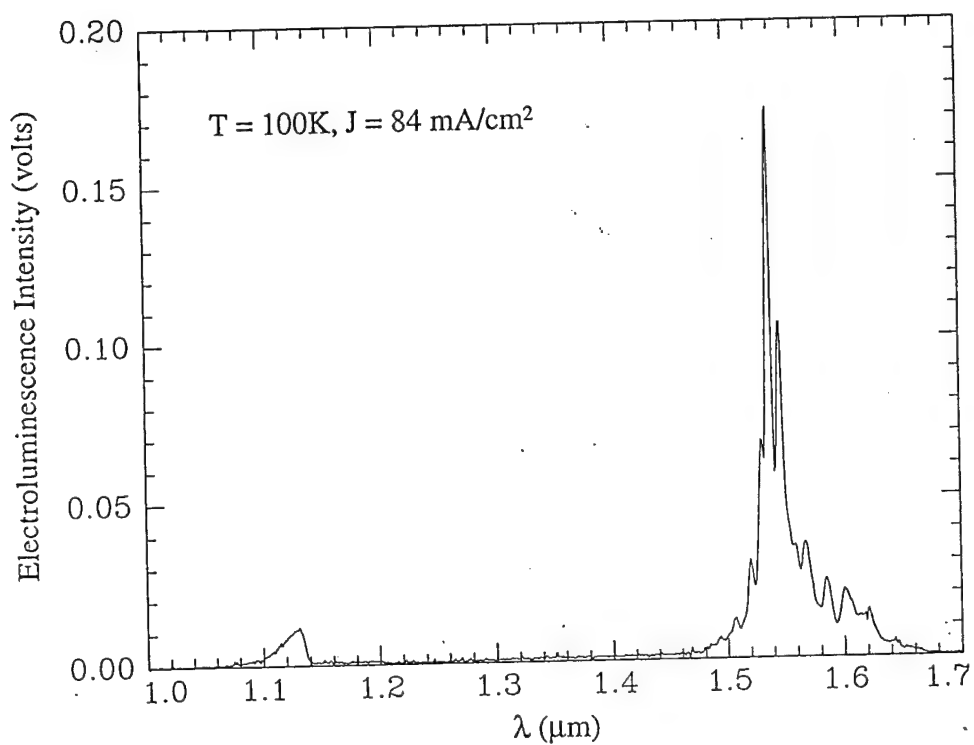


Figure 9. Electroluminescence spectrum of a 400 keV Si: Er LED at 100K.

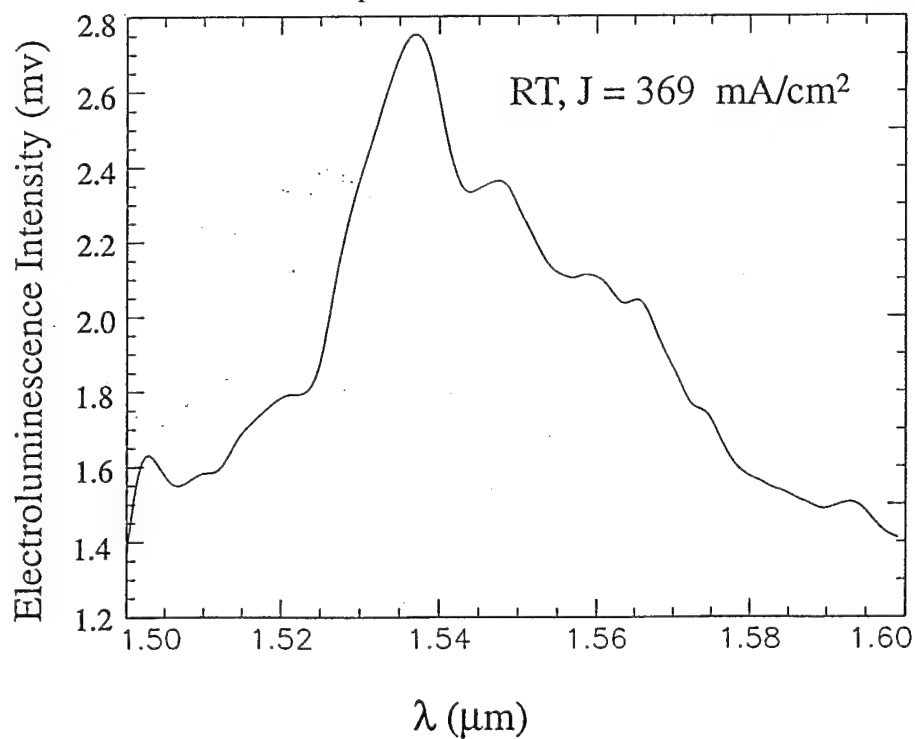


Figure 10. Electroluminescence spectrum of a 400 keV Si: Er LED at room temperature.

dependence on drive current density at both 100K and room temperature are shown in Fig. 11 and Fig. 12. At 100 K, the Er^{3+} EL intensity saturates at a drive current density of about 0.1 A/cm^2 , while it saturates at about 0.4 A/cm^2 at room temperature. At both 100 K and room temperature, the Er^{3+} EL intensity from 400 keV Si:Er LEDs saturates at a lower drive current density than for 4.5 MeV Si:Er LEDs. As a comparison, 4.5 MeV Er^{3+} EL intensity dependence on drive current density was also plotted in Fig 7. The improved current density dependence can be attributed to two factors: (1) 400 keV Er implantation has a smaller straggle and therefore a thinner implanted erbium region ($< 1500\text{\AA}$) compared to 4.5 MeV, and (2) the As emitter is very close to the Er region in the 400 keV case, a lower forward bias is needed to inject enough minority carriers to saturate the Er.

The EL intensity decreases significantly with temperature as shown in Fig 13. The EL peak intensity was monitored near its saturation value with a constant drive current density over the entire temperature range. A similar thermal quenching behavior is observed in the 4.5 MeV Si:Er LEDs.

The arsenic shallow emitter depth is a key design parameter for 400 keV Si:Er LEDs. The lower As implant energy and dose in the second lot creates a shallower As emitter. A shallower As emitter takes away less Er implanted region, more implanted Er is available for light emission, and therefore the Er^{3+} EL intensity increases as the As emitter depth decreases as shown in Fig 14. To further decrease the junction depth and to avoid spiking problems, a 3rd lot with a polysilicon emitter is underway. The polysilicon layer is deposited on a p-type substrate and implanted with phosphorus to form a n^+ layer. By diffusing phosphorus from the poly layer into the bulk silicon, a shallower and less defective n^+/p junction is expected.

A comparison of external quantum efficiency of 400 keV and 4.5 MeV Si:Er LEDs indicates that the external efficiency of a 400 keV Si:Er LED is about 3.5 times higher than 4.5 MeV LED. At room temperature and the same drive current density ($J = 0.5 \text{ A/cm}^2$), the Er^{3+} EL intensity of a 4.5 MeV LED is about 1.5 mV (from lock-in amplifier), while the intensity is about 0.5 mV for a 400 keV LED. However, the implanted Er dose at 400 keV is $3.5 \times 10^{12} \text{ cm}^{-2}$ compared to a $3.8 \times 10^{13} \text{ cm}^{-2}$ at 4.5 MeV. Therefore the ratio of the external efficiency of a 400 keV LED to a 4.5 MeV LED is estimated as,

$$\eta_{\text{ext}} (400 \text{ keV}) / \eta_{\text{ext}} (4.5 \text{ MeV}) = (0.5/1.5) * (3.8 \times 10^{13} / 3.5 \times 10^{12}) = 3.6$$

Less silicon damage associated with 400 keV Er implantation and an As emitter close to the Er region contribute to a higher Er pumping efficiency and therefore a higher η_{ext} .

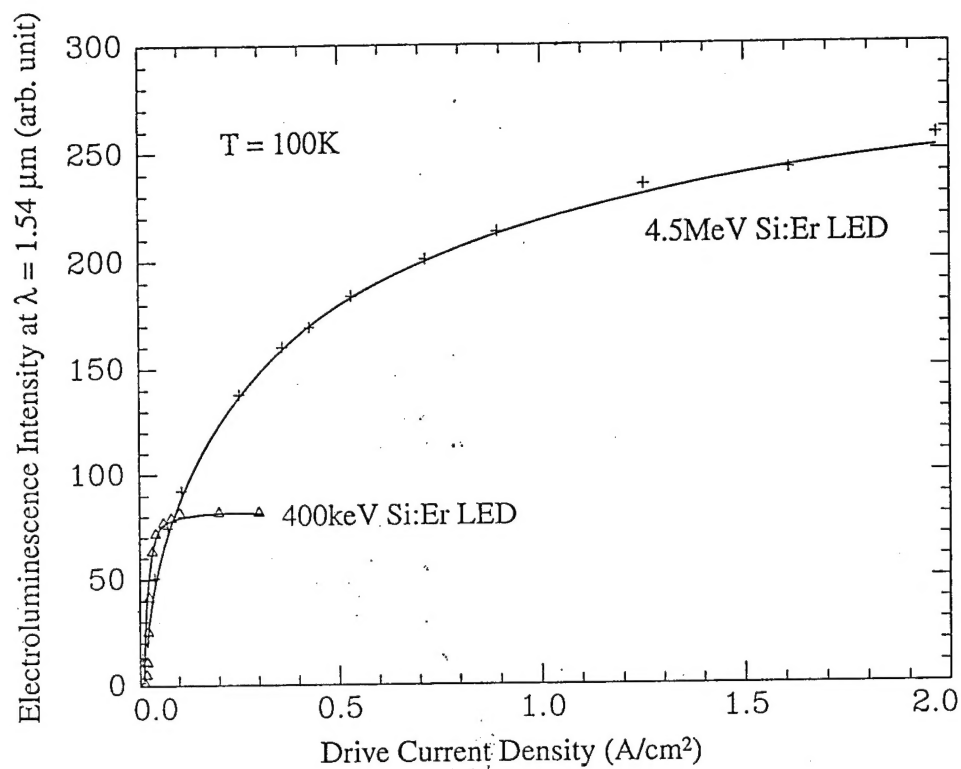


Figure 11. Er^{3+} electroluminescence intensity ($\lambda = 1.54 \mu\text{m}$) from both a 400 keV Si: Er LED and a 4.5 MeV Si: Er LED vs. drive current density at 100K.

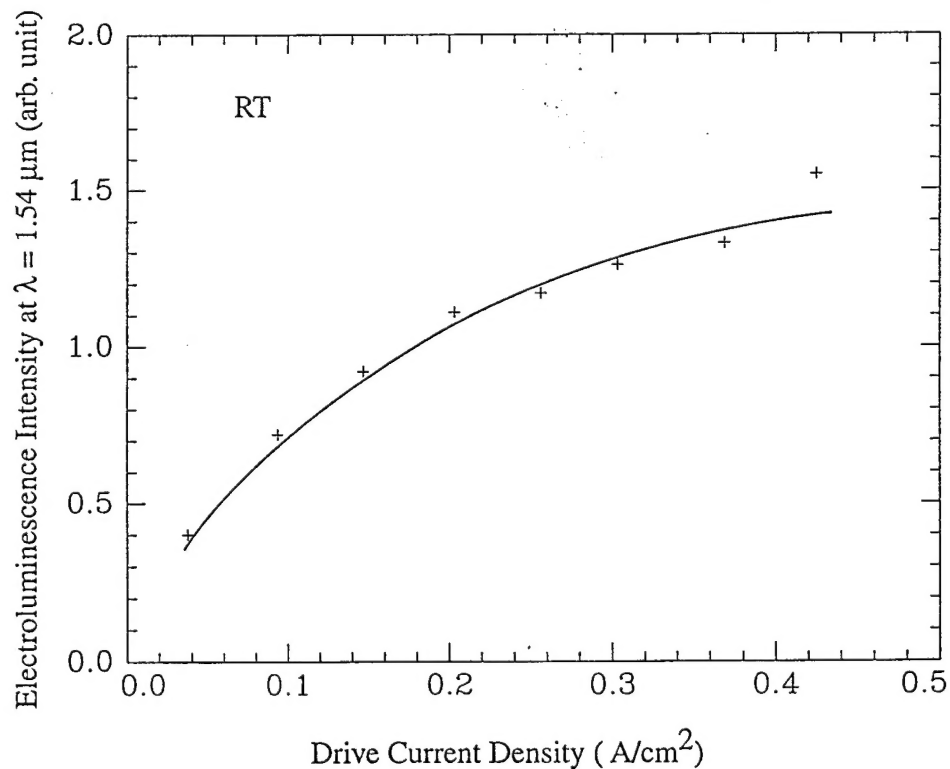


Figure 12. Er^{3+} electroluminescence intensity ($\lambda = 1.54 \mu\text{m}$) from both a 400 keV Si: Er LED and a 4.5 MeV Si: Er LED vs. drive current density at room temperature.

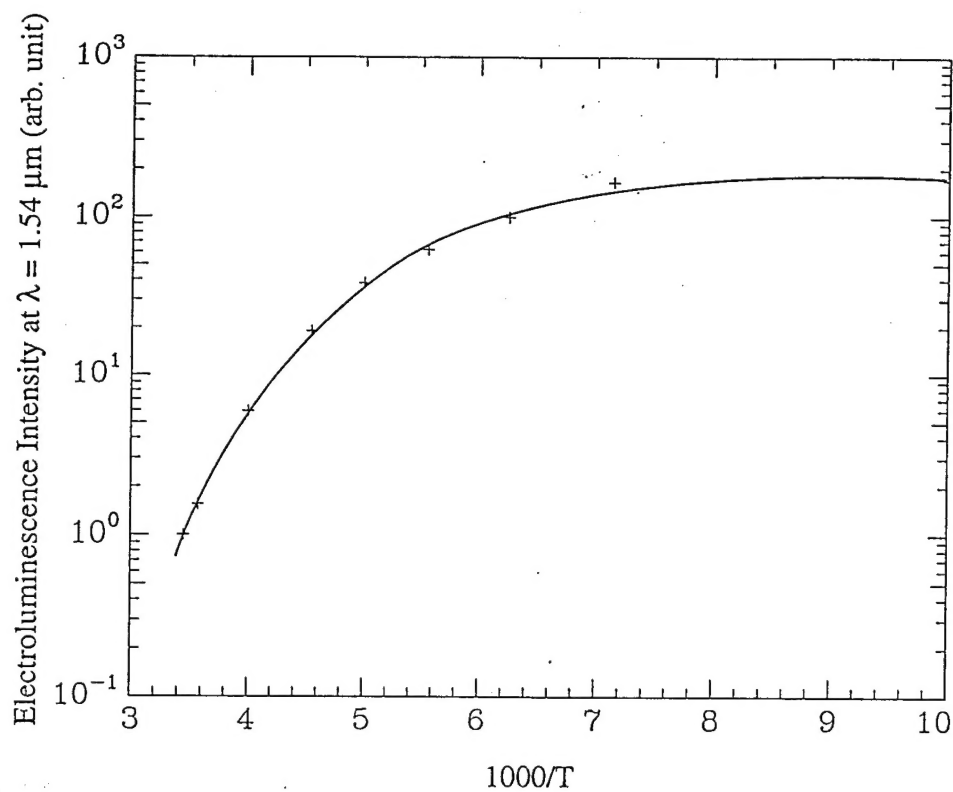


Figure 13. Temperature dependence of Er^{3+} electroluminescence intensity ($\lambda = 1.54 \mu\text{m}$) from a 400 keV Si: Er LED.

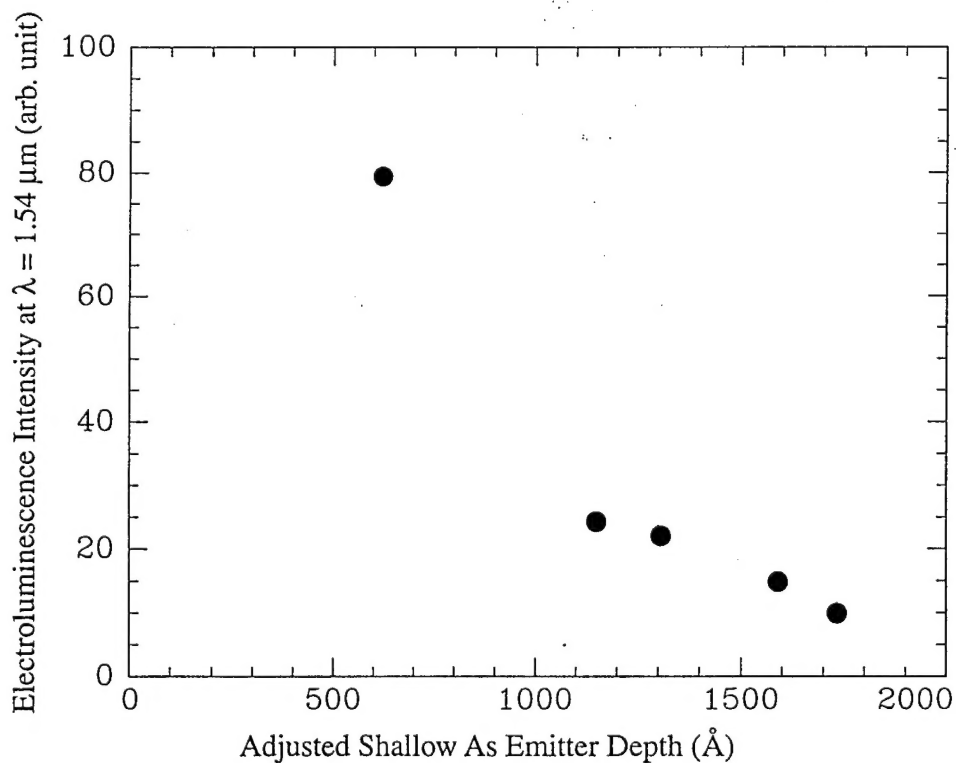


Figure 14. Shallow arsenic emitter depth dependence of Er^{3+} electroluminescence intensity ($\lambda = 1.54 \mu\text{m}$).

A second method to gauge device performance is to determine the percentage of optically active Er or internal quantum efficiency. This percentage can be estimated from the saturated Er emission output power. At 100 K, the Er saturation output power at $J = 0.1 \text{ A/cm}^2$ was estimated to be $P_{\text{out}} = 0.3 \text{ } \mu\text{W}$. At this drive current density, the Er^{3+} peak at $\lambda = 1.54 \text{ } \mu\text{m}$ is the main feature of the EL spectrum. The Er emission output power can be calculated as,

$$P_{\text{out}} = ([\text{Er}] * h * c) / (\tau_{\text{sp}} * \lambda)$$

where P_{out} is Er emission output power, $[\text{Er}]$ is the number of optically active Er atoms, and τ_{sp} is the spontaneous lifetime. Assuming $\tau_{\text{sp}} = 1 \text{ ms}$, we obtain $[\text{Er}] = 2.3 \times 10^9$ atoms. Given the Er implantation dose of $3.5 \times 10^{12} \text{ cm}^{-2}$ and a LED area of $9 \times 10^{-2} \text{ cm}^2$, in total dose*area = 3.1×10^{11} Er is implanted. Therefore, the percentage of optically active Er at 100 K can be estimated to be $2.3 \times 10^9 \text{ atoms} / 3.1 \times 10^{11} \text{ atoms} = 7.4\%$. Only about 1% of the Er is optically active at 100 K in the case of MeV implantation.

4.0 Suggestions for Continued Research

In order to completely integrate photonic and electronic signal processing on the microprocessor level, IC compatible processing methods must be developed to fabricate photonic devices in silicon. Results from this initial concept study clearly demonstrate the ability of Er ion implantation processing to create a photonic device in silicon. Several LED's were fabricated and evaluated at various temperatures. Room temperature emission was produced in the EL mode. Further work is necessary to better understand the mechanisms of the system and to develop optimized processing procedures.

The diodes made during the program exhibited high leakage current, further improvement can be made by making a better shallow junction and optimizing the device structure. The junction can be made by very low energy implantation (as performed), or the growth of a n+ top emitter. The deposition of a phosphorus doped polysilicon top emitter should create an excellent shallow junction, and should be performed in the phase II effort. The effects of out diffusion are significant and the process will require reduction in the thermal budget. Further investigation should be made into the use of multiple energy Er implants to yield a uniform distribution from the surface to a maximum depth. By uniformly doping as large a volume as possible, the emitted intensity can be improved since there is a greater number of emitting atoms present. By incorporating the above mentioned improvements, it is felt that emission intensity will be improve by several orders of magnitude.

While current technology iterates incremental improvements, silicon based optoelectronics represents a paradigm change. Materials development, system design and device prototyping are advancing to provide tools for the implementation of this technology. Continued research is required to fully develop the ability to monolithically integrate photonic and electronic processing.

References:

1. F.Y.G. Ren, J. Michel, Q. Sun-Paduano, B. Zheng, H. Kitagawa, D.C. Jacobson, J.M. Poate, and L.C. Kimerling. Mat. Res. Soc. Symp. Proc., 301 (1993) 87.
2. H. Ennen, J. Schnieder, G. Pomrenke, A. Axmann, Appl. Phys. Lett. 43 (1983) 943.
3. J.K. Hirvonen et al, "Production of High Current Metal Ion Beams," Proc. 3rd Int'l Conf. on Ion Implantation, Kingston, Ont., July 1980.
4. S.N. Bunker and A.J. Armini, Nucl. Instr. and Meth. B, 39 (1989) 7.